PROGRESS IN COLOR, COLORANTS AND COATINGS

available online @ www.pccc.icrc.ac.ir

Progress in Color Colorants Coating 18 (2025), 145-162

Ministry of Science, Research and Technology
Institute for Color Science & Technology

Optical and Morphological Properties of Poly(vinyl chloride) Thin Films with Organic Content Reinforced by Nanoparticles Embedded which is Freestanding

R.N. Abed[*1], E. Yousif[2], M. H. Rahman[3], M. Kadhom[4], A. Basem[5], H. Hashim[6]**

[1.] Department of Mechanical Engineering, College of Engineering, Al-Nahrain University, P.O. Box: 64040, Jadriyah, Baghdad, Iraq.
[2.] Department of Chemistry, College of Science, Al-Nahrain University, P.O. Box: 64021, Jadriyah, Baghdad, Iraq
[3.] Aeronautical Technical Engineering, Al-Farahidi University, P.O. Box: 10011, Baghdad, Iraq
[4.] Department of Environmental Science, College of Energy and Environmental Sciences, Al-karkh University of Science, Baghdad, 10080, Iraq
[5.] Air conditioning Engineering, Faculty of Engineering, Warith Al-Anbiyaa University, Karbala 56001, Iraq
[6.] Department of Physics, College of Science, Al-Nahrain University, Baghdad 64021, Iraq

ARTICLE INFO

Article history:
Received: 28 Apr 2024
Final Revised: 20 June 2024
Accepted: 23 June 2024
Available online: 25 Sept 2024

Keywords:
Poly(vinyl chloride)
Organic compound (Domperidone)
Optical conductivity
Urbach energy
Roughness

ABSTRACT

Newly modified poly(vinyl chloride) nanocomposite thin films incorporating domperidone as an organic compound and doped with NPs (Co_3O_4, NiO, and Cr_2O_3) were fabricated using the casting method. PVC was modified with 25 g of the organic material domperidone (PVC/D) and subsequently doped with 0.01 g of Co_3O_4, NiO, and Cr_2O_3 NPs to create the modified nanocomposite thin films, PVC/D/Co_3O_4, NiO, and Cr_2O_3, the NPs dimeters was < 50 nm. These films were investigated using diffusive reflectance within the 250-1350 nm wavelength range. The X-ray diffraction (XRD) analysis revealed a semi-crystalline structure for the modified PVC. The optical properties of the modified nanocomposite thin films were assessed, resulting in decreased transmittance and reflectance values, with absorption coefficients ranging from 88 to 94 %. Upon NP doping, the nanocomposite thin films' direct and indirect energy band gaps decreased from 4.7 to 3.0 and 4.3 to 2.9 eV, respectively. This decrease was attributed to an increase in localized states, leading to higher disorder within the material following an increase in Eu from 0.862 to 3.096 eV. Scanning electron microscopy (SEM) analysis illustrated the nanocomposite structure of modified PVC. In contrast, the measurements of atomic force microscopy (AFM) indicated increased surface roughness from 2.31 nm to 6.16 nm for the modified PVC thin films. These modified PVC nanocomposite thin films find potential applications in various industries, including air transport components, light-emitting diodes, laser sensors, UV energy shielding, light-harvesting devices, memory devices, and light-conversion technologies. Prog. Color Colorants Coat. 18 (2025), 145-162© Institute for Color Science and Technology.

1. Introduction

Poly(vinyl chloride) (PVC), a plastic material, is known for its inherent limitations, characterized by low thermal stability and subpar mechanical properties. Consequently, considerable efforts have been directed towards enhancing PVC's robustness, particularly in the face of elevated temperatures, through applying organic compounds and nanomaterials. As a result, the researchers focused on modifying PVC due to its significant structural properties. The two primary

*Corresponding author: * Rasheed N. Abed: rasheed.n.abed@nahrainuniv.edu.iq
**Emad Yousif: emad_yousif@hotmail.com
https://doi.org/10.30509/pccc.2024.167313.1300

approaches of filling NPs and adding organics were pursued to improve this polymer, often leading to development of compounds with favorable properties for PVC modification [1, 2]. These enhancements serve to fortify the PVC structure through the integration of either nanoparticles or organic materials.

The first process involved using organic materials in PVC composites. Various organic compounds were combined with PVC to aid in its modification. These compounds are represented in multiple amino derivatives, such as thiazole, imidazole, pyrimidine, nitroaniline, and dichloroaniline [3, 4]. Furthermore, Schiff bases contain the 1,2,4-triazole ring in conjunction with Copper (II) chloride ($CuCl_2$), which is also included [5]. Additionally, compounds like 1,3,4-thiadiazole with 1,3,4-oxadiazole [6], pyridine-4-carbohydrazide [7], phthaloyl groups in tandem with 1,3,4-thiadiazole [8], 4-amino-5-(3,4,5-trimethoxiy-phenyl)-1,2,4-triazole-2-thiol (0.2 g, 0.7 mmol) [9], 2-amino acetate benzothiazole [10], Schiff bases with $CuCl_2$ [11], 4-Amino-5-phenyl-4H-1,2,4-triazole-3-thiol (2) [12], and amino groups combined with aromatic aldehydes [13] are utilized to modify PVC.

The second process involves introducing various dopants into the PVC matrix, transforming its structure into a novel composite by incorporating nanoparticles (NPs). These compounds are intentionally chosen for their capacity to bestow advantageous properties upon PVC and are strategically combined with NPs to achieve desired outcomes. The escalating demand for various electronic devices, optical components, transistors, and magnetic applications has driven the interest in polymer nanocomposites. These applications stand out for their exceptional electrical and luminescent properties [14]. Many NPs have been systematically integrated into polymer matrices to meet this demand. These nanoparticles encompass zinc oxide (ZnO) [15], lead oxide (PbO) [16], chromium oxide (Cr_2O_3) [17], carbon nanotubes (CNT) combined with graphene [18], multi-wall carbon nanotubes (MWCNT) [19], titanium dioxide (TiO_2) [20], as well as diverse metal oxides like aluminum oxide and silicon dioxide (Al_2O_3 and SiO_2) [21], and kaolinite nanocomposites [22]. Furthermore, salts, including KnO_3, $CuCl_2$, and $MgCl_2$ [12, 23, 24], have been effectively harnessed to reshape PVC into nano-composite structures.

These innovations have significantly reinforced PVC structures, whether incorporating NPs, organic materials, or a combination of both. This has given rise to novel composites that are useful in numerous applications. Introducing chemical modifications and additives that bring about structural changes in polymers represents a valuable technique. This approach not only induces alterations in the chemical structure of the PVC backbone but also leads to notable enhancements in the photochemical properties of PVC. It is imperative to include appropriate stabilizers to counteract PVC degradation during thermal or photolytic treatments, with these additives effectively absorbing harmful UV radiation and curtailing photo-oxidation in polymeric materials [25, 26].

Hence, in the current study, an organic compound (domperidone) was introduced as an additive to PVC, serving as an organic material to enhance the material's electrical conductivity. This organic material is a novel choice for modifying PVC, given its possession of hydroxyl and carbonyl functional groups that can effectively alter the PVC's chemical bonds. Subsequently, we introduced NPs, specifically Co_3O_4, NiO, and Cr_2O_3, in a subsequent stage to modify the PVC structure further after its interaction with domperidone. Combining these nanoparticles with domperidone is intended to augment PVC's conductivity and facilitate the creation of a novel structure characterized by a reduced energy gap [25].

The primary objective of this study is to produce PVC samples initially modified with domperidone, referred to as PVC/D. Following this initial modification, the next step involved doping the modified PVC with NPs, namely Co_3O_4, NiO, and Cr_2O_3 (referred to as PVC/D/Co_3O_4, PVC/D/NiO, and PVC/D/Cr_2O_3, respectively). This synergizing aimed to improve the light resistivity exhibited by these materials. Furthermore, X-ray diffraction (XRD) testing is employed to discern whether the PVC structure has acquired crystalline or non-crystalline characteristics. To gain insights into the microstructure, scanning electron microscopy (SEM) is used to visualize the PVC structure, while atomic force microscopy (AFM) quantifies the surface roughness of the thin films. The nanocomposite thin films of modified PVC generated in this study hold promise for various industries, including applications in air transport, light-emitting diodes, laser sensors, UV energy shielding, light-harvesting devices, memory devices, and light-conversion technologies.

2. Experimental

2.1. Materials

The PVC material was procured from PetKim Petrokimya company in Istanbul, Turkey. The nanoparticles (Co_3O_4, NiO, and Cr_2O_3) were obtained from Changsha Easchem company in Hunan, China. These nanoparticles boast a remarkable purity level of 99 %, and their detailed characterization is presented in Table 1.

2.2. Test equipment

Several essential pieces of equipment were employed in the experimental work. The Avantes UV-Visible Spectro (UV-Visible-2048, DH-S-BAL-2048) was central in collecting data samples, covering incident wavelengths from 250 to 1300 nm with a step size of 0.5 nm. The SEM was used to examine the morphology of the thin films within the nanocomposite materials. The AFM model AA2000 facilitated the roughness measurement for the blank PVC and the nano-composite thin films. Additionally, a Micrometer type 2610 A, manufactured in Germany, was utilized to determine the thickness of the nanocomposite thin films. These instruments collectively contributed to the successful execution of the experiments and the characterization of the materials under investigation.

2.3. Blank PVC thin film preparation

The preparation of thin, blank PVC films involved several steps. Initially, 6 grams of blank PVC were dissolved in 100 mL of tetrahydrofuran (THF), serving as the solvent. This solution was stirred for 4 hours at 25 °C. Subsequently, the mixture was subjected to sonication for 1 hour to eliminate any trapped air bubbles. The resulting solution was then carefully poured into a clean glass template with a thickness of 40 µm. The template was left undisturbed for a day to allow for the gradual evaporation of THF. To ensure the removal of any residual solvent, the PVC films were further dried in a vacuum oven at 40°C for 6 hours. Following this, the PVC thin film was fabricated using the casting method.

2.4. Preparation of modified PVC thin film with domperidone

25 mg of organic compound (domperidone) was introduced to 6 grams of PVC to create modified PVC thin films. This resulted in modifying PVC thin films by incorporating domperidone as an organic material cluster.

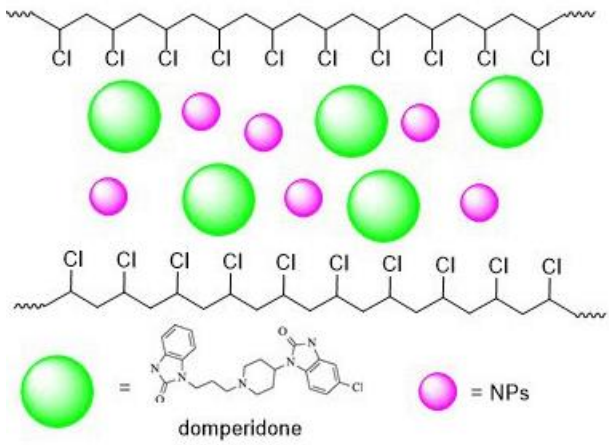

Scheme 1: Synthesis of domperidone-enhanced PVC nanocomposite thin films via NPs doping.

Table 1: Data of utilized NPs.

No.	NPs type	Supplier	Purity (%)	Size of particles (nm)
1	Co_3O_4	Changsha Easchem company /Hunan/China	99.98	15
2	NiO	Changsha Easchem company /Hunan/China	99.98	15
3	Cr_2O_3	Changsha Easchem company /Hunan/China	99.98	18

2.5. Preparation of modified PVC thin films doped with nanoparticles

A portion of the PVC thin films modified with domperidone was further enriched by adding small quantities (0.1 % wt.) of NPs, specifically Co_3O_4, NiO, and Cr_2O_3. This process aimed to create thin films of doped modified PVC nanocomposite. The mixture was thoroughly blended for 2 hours using a stirrer device. Subsequently, the resulting mixture was carefully poured onto a glass template. These samples were then placed in a semi-circular glass container to dry, ensuring the removal of any residual solvent, and left undisturbed for 24 hours. The thickness of the resulting samples was maintained at 40 µm. Scheme 1 illustrates the modified PVC with an organic compound (domperidone) and doped by NPs, where the NPs are dangled between the PVC series.

3. Results and Discussion

The results and discussion demonstrated the effect of domperidone on modifying PVC and the impact of doping the polymer with Co_3O_4, NiO, and Cr_2O_3 NPs to enhance its optical properties for light conversion applications. The data on optical properties were interpreted and analyzed, and the Urbach energy was also computed.

3.1. XRD

The XRD test was conducted to elucidate the structural changes in PVC before and after modification with domperidone and the following NPs filling. Figure 1 provides insight into the structural characteristics of pristine PVC, domperidone-modified PVC (PVC/D), and PVC nanocomposite films (PVC/D/Co_3O_4, NiO, and Cr_2O_3). Figure 1 revealed a semi-crystalline structure after introducing the domperidone and NPs into the PVC matrix.

Figure 1 illustrates distinctive features for each of the samples. The modified PVC (PVC/D) displays a single peak at an angle of 26°. In contrast, the modified PVC/Co_3O_4 exhibits two distinct features: a pronounced hump at 15° and a peak at 26°. Similarly, modified PVC/NiO showcases a single peak at 26°. For modified PVC/Cr_2O_3, two characteristics are evident: a minor hump at 15° and a peak at 26°. The shared presence of these structural elements indicates a semi-crystalline nature in the synthesized materials [25].

3.2. Reflection test of PVC thin films

Figure 2 presents the results of the reflectance test conducted on pristine PVC, domperidone-modified PVC (PVC/D), and PVC nanocomposite thin films (PVC/D/Co_3O_4, NiO, and Cr_2O_3) following the addition of NPs. From the figure, it is evident that the reflectance (*R*) values of all the PVC samples decreased from a high value of 0.6 within the region (380>λ>300 nm) to a lower value of 0.11. Subsequently, the reflectance gradually increases within the region (480>λ>360 nm) for blank PVC, PVC/D/Co_3O_4, and PVC/D/NiO. However, for samples PVC/D and PVC/D/Cr_2O_3, the reflectance increases in the region (560>λ>420 nm), reaching values ranging from 0.06 to 0.17, which remain relatively constant. Consequently, Figure 2 illustrates that the addition of domperidone and NPs leads to a reduction in the reflectance (*R*) values.

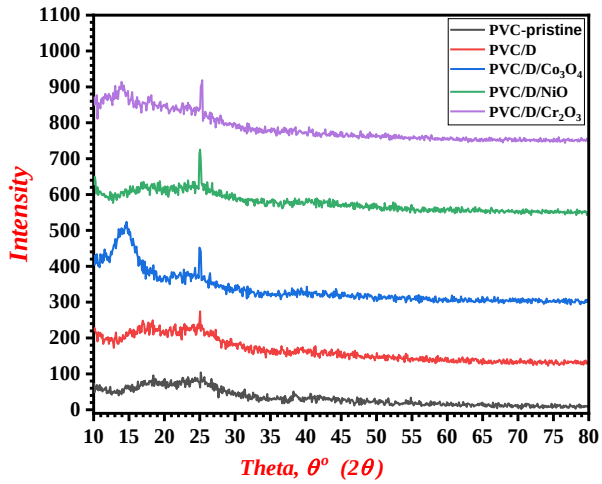

Figure 1: XRD test for pristine PVC, modified PVC/D, and PVC/D/NPs.

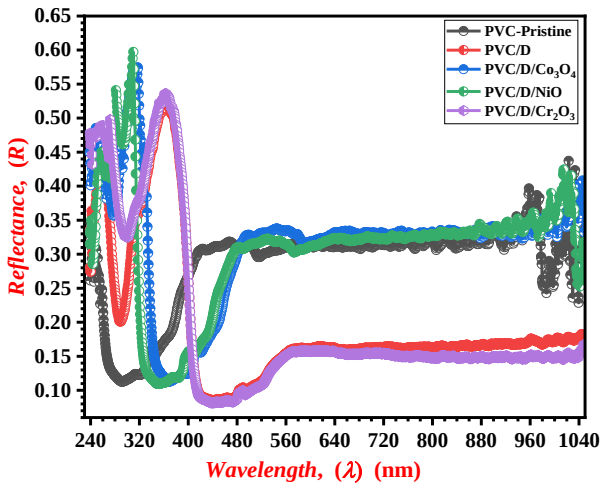

Figure 2: Reflectance test for pristine PVC, modified PVC/D, and PVC/D/NPs.

The observed increases in reflectance (*R*) values for PVC/D/Co_3O_4 and PVC/D/NiO within specific regions can be attributed to factors like inhomogeneous blending and the distinct features of these materials. Consequently, the absorption coefficient values lie within the 88-94 % [26, 27].

3.3. Absorption coefficient of PVC thin films

The absorption coefficient (α) is a fundamental parameter within the optical system, playing a pivotal role in elucidating the electronic properties and mobility characteristics across the valence and conduction bands in a composite material. This absorption energy arises from the incident wavelength's interaction with the particle structure, imparting the requisite energy to electrons, thus facilitating their transitions between energy states [28, 29].

Figure 3 reveals the absorption coefficient (α) values for pristine PVC, domperidone-modified PVC (PVC/D), and PVC nanocomposites (PVC/D/Co_3O_4, NiO, and Cr_2O_3). These values provide valuable visions into the electronic nature and mobility within these materials, reflecting the influence of organic compounds (domperidone) and the incorporated NPs on the absorption characteristics.

The absorption coefficient (α) is intricately linked with the absorbance values and can be calculated using equation 1 [28, 29].

$$\alpha = 2.303 \times \frac{A}{t} \qquad (1)$$

where α represents the absorption coefficient in cm^{-1}, A represents the absorbance value, and t denotes the coating thickness in centimeters (cm).

As illustrated in Figure 3, the absorption coefficient (α) curves are provided for pristine PVC, domperidone-modified PVC (PVC/D), and PVC nanocomposites (PVC/D/Co_3O_4, NiO, and Cr_2O_3). Adding an organic compound (domperidone) to modify PVC and the subsequent doping of PVC with NPs increases the absorption coefficient (α). Within the UV region, α exhibits fluctuations with low and high magnitudes. However, these magnitudes rise and stabilize within the visible region, with some fluctuations observed along the wavelength axis as it increases [29]. This data elucidates the changes in the absorption characteristics, underscoring the impact of organic compound (domperidone) and NPs doping on the absorption coefficient (α) of the materials under investigation.

3.4. Transmittance of PVC thin films

The transmittance (*T*) values for pristine PVC, domperidone-modified PVC (PVC/D), and PVC nanocomposites (PVC/D/Co_3O_4, NiO, and Cr_2O_3) are presented in Figure 4. These transmittance values range from 0.14 to 0.26, indicating the extent to which light is transmitted through the PVC composites. Figure 4 reveals notable characteristics in the transmittance (*T*) values. Within the UV region (240≤λ≤380 nm), the transmittance values exhibit fluctuations and instability. In contrast, within the visible region (400≤λ≤800 nm), the transmittance (*T*) values decline and subsequently stabilize, maintaining a continuous pattern. Consequently, Figure 4 underscores that the PVC nanocomposites exhibit reduced transmittance (*T*) values following the addition of NPs (Co_3O_4, NiO, and Cr_2O_3) to the domperidone-modified PVC [30, 31].

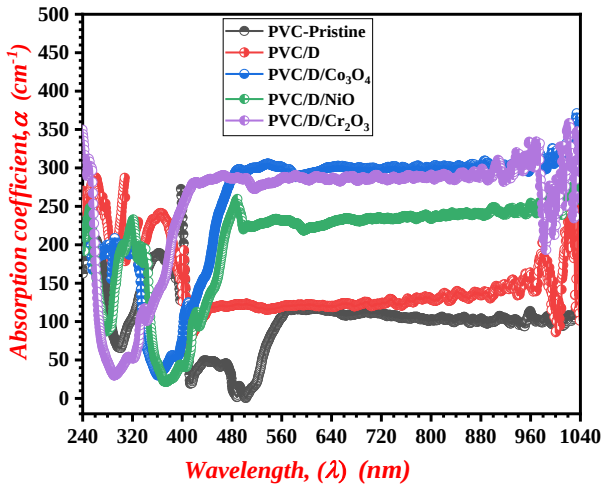

Figure 3: Absorption coefficient for pristine PVC, modified PVC/D, and PVC/D/NPs.

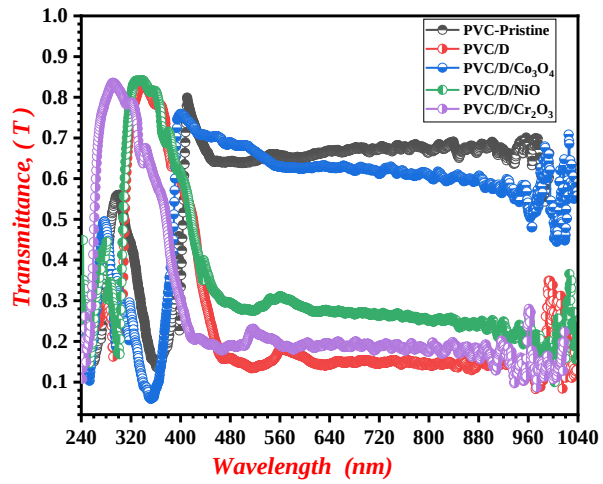

Figure 4: Transmittance for pristine PVC, modified PVC/D, and PVC/D/NPs.

3.5. Skin depth of PVC thin films

When host materials are introduced, or any thin film coating incorporates these host materials, the absorption of light rises. The skin depth (x) is a characteristic that relates to absorbance and relies on the incident wavelength (λ) and the extinction factor (k).

The calculation of the skin depth (x) can be achieved using equation 2 [32].

$$x=\frac{\lambda}{2\pi k} \quad (2)$$

In this equation, x represents the skin depth in nanometers (nm), λ represents the wavelength in nanometers (nm), and k denotes the extinction factor. Figure 5 provides an illustration of the skin depth (x) for pristine PVC, domperidone-modified PVC (PVC/D), and PVC nanocomposites (PVC/D/Co_3O_4, NiO, and Cr_2O_3).

As depicted in Figure 5, the skin depth (x) provides insights into the absorption properties of these PVC composites. Notably, the skin depth (x) increases within the wavelength range of 240≤λ≤520 nm. This phenomenon is best explained by examining the inset Figure 5, which elucidates each curve's skin depth (x) peaks and reveals distinct *cut-off* wavelengths. In the case of domperidone-modified PVC (PVC/D), a peak is observed within the region of 400≤λ≤420 nm, referred to as the *cut-off* wavelength ($E_{cut\text{-}off}$). Similarly, for modified PVC nanocomposites (PVC/D/Co_3O_4 and NiO), peaks are observed in the region of 340≤λ≤480 nm, also corresponding to *cut-off* wavelengths ($E_{cut\text{-}off}$). However, for the modified PVC nanocomposite (PVC/D/Cr_2O_3), a peak is observed in the 260≤λ≤400 nm region, marking its cut-off wavelength.

During these *cut-off* wavelength periods ($E_{cut\text{-}off}$), absorbance essentially vanishes, and these peaks decline as the wavelength increases beyond these specific ranges. Introducing nanoparticles into PVC results in the darkening of the nanocomposite thin films, ultimately leading to higher absorption values for these materials [32, 33]. These observations highlight the role of organic compounds (domperidone) and nanoparticles in influencing the skin depth and absorption characteristics of PVC composites.

3.6. Refractive index of PVC thin film

The refractive index (n) holds great significance, particularly concerning the polarized electrons within thin films. Figure 6 displays the refractive index (n) values for pristine PVC, domperidone-modified PVC (PVC/D), and PVC nanocomposites (PVC/D/Co_3O_4, NiO, and Cr_2O_3). The refractive index (n) can be calculated using equation 3 [33].

$$n=\left[\frac{1+R}{1-R}\right]+\sqrt{\frac{4R}{(1-R)^2}-k^2} \quad (3)$$

where n is the refractive index, R is reflectance, and k is the extinction factor. Figure 6 illustrates the refractive index (n) values for these materials. Notably, the refractive index exhibits higher values within the UV region (λ<400 nm).

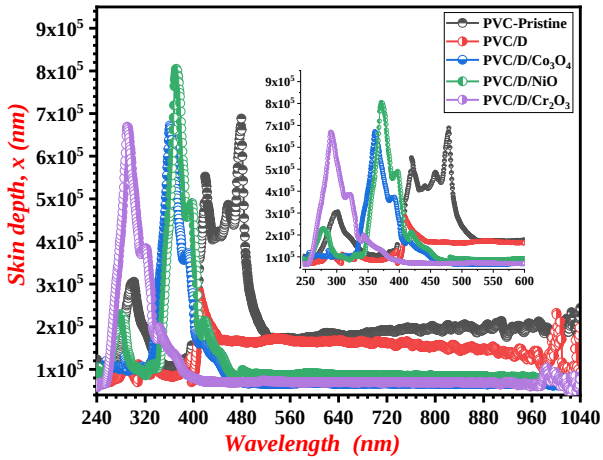

Figure 5: Skin depth (x) for pristine PVC, modified PVC/D, and PVC/D/NPs.

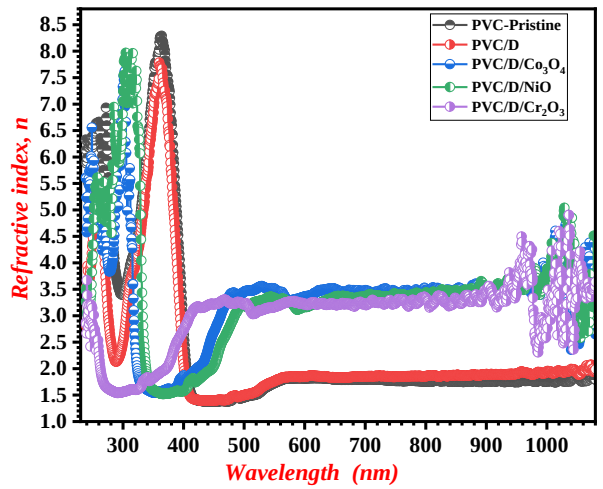

Figure 6: Refractive index (n) for pristine PVC, modified PVC/D, and PVC/D/NPs.

This phenomenon is attributed to the impact of incident wavelengths on electron orbit interactions, resulting in electron polarization. However, the curves become continuous and stable within the visible region (λ>400 nm). The refractive index (*n*) attains a high value of n=3.6 after adding NPs (Co_3O_4, NiO, and Cr_2O_3) to the domperidone-modified PVC. These results indicate a significant decrease in the speed of light as it passes through the nanocomposite thin films. The refractive index (*n*) values thus provide crucial information about the behavior of light within these materials and the impact of NPs doping on their optical properties [33].

3.7. Extinction factor of PVC thin film

The extinction factor (*k*) pertains to the attenuation of electromagnetic waves within thin films, reflecting the loss in absorbance and the extent of light absorption. It describes the phenomenon where some wavelengths of light are absorbed while the rest are reflected from the particle's surface, and this interaction depends on the incident wavelength angle.

The extinction factor (*k*) can be calculated using equation 4 [34].

$$k = \frac{\alpha\lambda}{4\pi} \quad (4)$$

In this equation, α represents the absorption coefficient in cm^{-1}, and λ is the wavelength in nanometers (nm). Figure 7 provides an overview of the extinction factor (*k*) for pristine PVC, domperidone-modified PVC (PVC/D), and PVC nanocomposites (PVC/D/Co_3O_4, NiO, and Cr_2O_3).

As previously reported, the extinction factor (*k*) measures the losses in absorbance. Figure 7 demonstrates the losses in absorbance for pristine PVC, domperidone-modified PVC (PVC/D), and PVC nanocomposites (PVC/D/Co_3O_4, NiO, and Cr_2O_3). Notably, these losses are exceptionally small, with values ranging in the order of thousandths. The highest recorded value is 0.0028, which is still remarkably small. This indicates that these nanocomposites of modified PVC exhibit high absorbance characteristics, emphasizing their capacity to effectively absorb electromagnetic waves and light, which aligns with previous studies [34, 35].

3.8. Optical conductivity of PVC thin films

The optical conductivity (*σ*) relates to the conductance inside these thin films, allowing electrons to move through the band levels (valence and conduction). This conductivity arises after a portion of the incident wavelength light is absorbed, with electrons leaving behind holes in the valence band, enabling conductivity within the thin films.

The computation of optical conductivity (*σ*) can be achieved using equation 5 [36].

$$\sigma = \frac{\alpha n c}{4\pi} \quad (5)$$

Here, *σ* represents the optical conductivity (*σ*) in S^{-1}, *α* is the absorption coefficient in cm^{-1}, *n* is the refractive index, and c is the speed of light (approximately 3×10^{10} cm/s) [37, 38]. Figure 8 presents an overview of the optical conductivity (*σ*) values for pristine PVC, domperidone-modified PVC (PVC/D), and PVC nanocomposites (PVC/D/Co_3O_4, NiO, and Cr_2O_3).

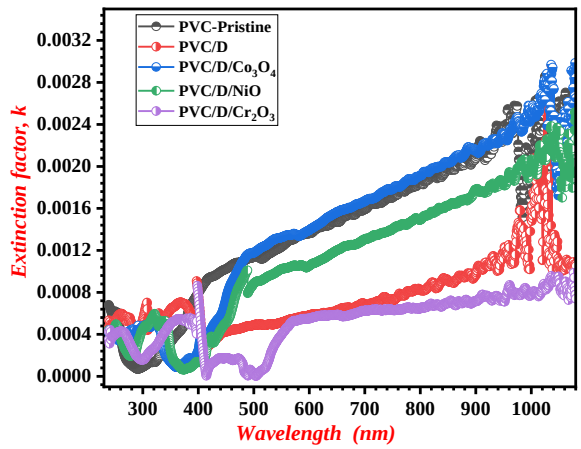

Figure 7: Extinction factor (*k*) for pristine PVC, modified PVC/D, and PVC/D/NPs.

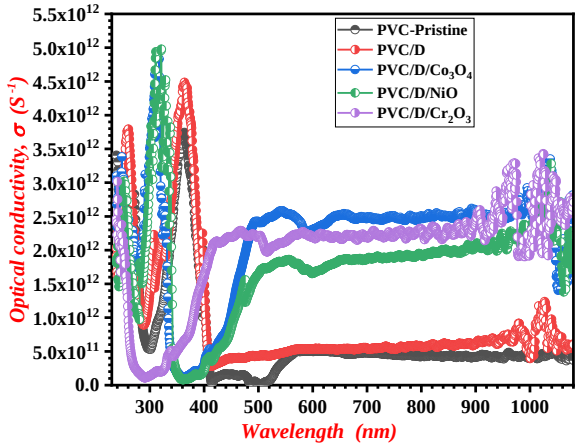

Figure 8: Optical conductivity (*σ*) for pristine PVC, modified PVC/D, and PVC/D/NPs.

Figure 8 clearly illustrates that the optical conductivity (σ) for pristine PVC, domperidone-modified PVC (PVC/D), and PVC nanocomposites (PVC/D/Co_3O_4, NiO, and Cr_2O_3) increases significantly after the addition of NPs (Co_3O_4, NiO, and Cr_2O_3) to the modified PVC. The highest recorded value of optical conductivity (σ) is 2.6×10^{12} S^{-1} after incorporating NPs. These NPs play a crucial role in enhancing the structure of modified PVC, transforming it into a nanocomposite with notable conductance properties. This increase in optical conductivity (σ) indicates that these materials effectively facilitate electron transit through the band levels, contributing to their conductive characteristics [39].

3.9. Dielectric constant of PVC thin films

The dielectric constant (Ɛ) reflects the mobility of free electrons within the material, and the generation of charges depends on electrons transitioning from the valence band to the conduction band. This property is crucial in understanding the charge carriers within polymers and can be categorized into real ($Ɛ_1$) and imaginary ($Ɛ_2$) dielectric constants. Equation 6 is employed to calculate the dielectric constant, with the components of the equation related to the refractive index (n) and the extinction factor (k) [39].

$$[(Ɛ)= Ɛ_1(\omega)+i\, Ɛ_2(\omega)] \quad (6)$$

The real ($Ɛ_1$) and imaginary ($Ɛ_2$) dielectric constants can be determined using equation 7 [40]:

$$\begin{bmatrix} \varepsilon_1=n^2-k^2 \\ \varepsilon_2=2nk \end{bmatrix} \quad (7)$$

Figures 9 and 10 depict the real ($Ɛ_1$) and imaginary ($Ɛ_2$) dielectric constants for pristine PVC, domperidone-modified PVC (PVC/D), and PVC nanocomposites (PVC/D/Co_3O_4, NiO, and Cr_2O_3). Figure 9 specifically illustrates the real dielectric constant ($Ɛ_1$) for pristine PVC, domperidone-modified PVC, and PVC nanocomposites.

Figure 9 demonstrates the behavior of the real dielectric constant ($Ɛ_1$) for pristine PVC, domperidone-modified PVC (PVC/D), and PVC nanocomposites (PVC/D/Co_3O_4, NiO, and Cr_2O_3). The real dielectric constant ($Ɛ_1$) increases significantly after adding NPs (Co_3O_4, NiO, and Cr_2O_3) to the modified PVC. This observation indicates that the thin films exhibit high absorption [41].

In Figure 10, the imaginary dielectric constant ($Ɛ_2$) is illustrated for the same materials: pristine PVC, domperidone-modified PVC (PVC/D), and PVC nanocomposites (PVC/D/Co_3O_4, NiO, and Cr_2O_3). The imaginary component of the dielectric constant ($Ɛ_2$) reflects the losses in absorption within these materials [42].

Figure 10 indicates the behavior of the imaginary dielectric constant ($Ɛ_2$) for pristine PVC, domperidone-modified PVC (PVC/D), and PVC nanocomposites (PVC/D/Co_3O_4, NiO, and Cr_2O_3). The values of the imaginary component are very small, on the order of a part in thousands. This observation suggests that the losses in absorption for the PVC nanocomposite thin films are minimal. Such losses are typically generated by the electric dipoles of atoms undergoing polarization under the influence of an electric field [43].

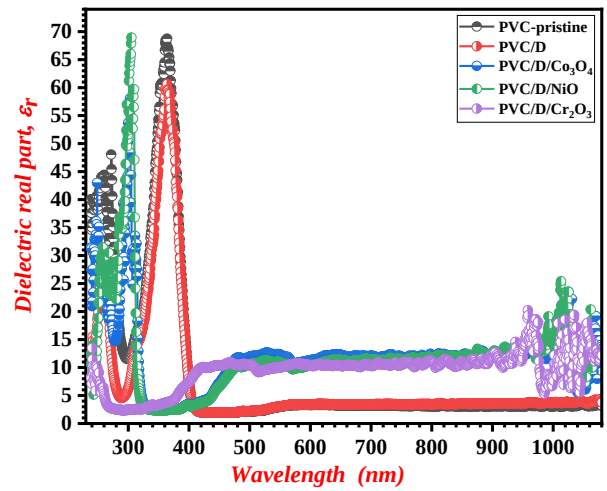

Figure 9: Real dielectric constant for pristine PVC, modified PVC/D, and PVC/D/NPs.

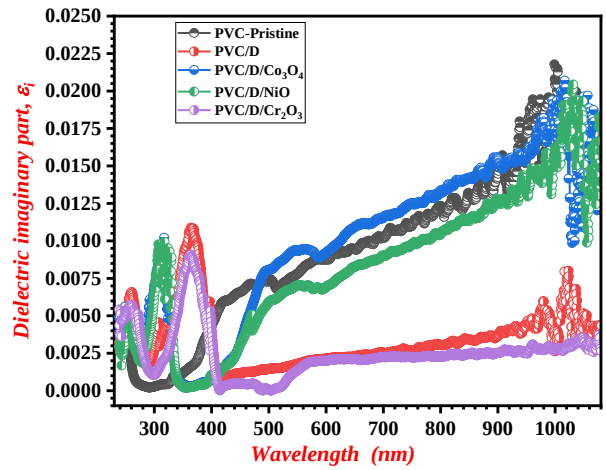

Figure 10: Imaginary dielectric constant for pristine PVC, modified PVC/D, and PVC/D/NPs.

3.10. Optical energy gap of PVC thin films

The materials' optical energy gap (Eg) provides insight into the energy required for electrons to transition from the valence band to the conduction band, indicating their absorbance energy [35]. Tauc's relation 8 is commonly employed to calculate this energy gap. It relates the absorption coefficient (α) to the photon energy ($h\nu$), where α is raised to the power of 1/n, with n representing the transition type (n=2 for indirect transitions and n=0.5 for direct transitions). The constant B is specific to semiconductors [44].

$$\alpha h\nu^{1/n}=B\left(h\nu-E_g\right) \quad (8)$$

In Figure 11, the direct transition energy gap for pristine PVC, domperidone-modified PVC (PVC/D), and PVC nanocomposites (PVC/D/Co_3O_4, NiO, and Cr_2O_3) is illustrated. To determine the energy gap for both direct and indirect transitions, one can plot the square of the photon energy $(\alpha h\nu)^2$ against the photon energy ($h\nu$) and extrapolate the line to where $(\alpha h\nu)^2$ equals zero. This method allows for determining the energy gap for different transition types.

As shown in Figure 11, the direct transition optical energy gap (E_g) varies for different materials: pristine PVC (E_g=4.7 eV), PVC+D (E_g=3.0 and 4.0 eV), PVC+Co_3O_4 (E_g=3.6 and 4.2 eV), PVC+NiO (E_g=3.5, 3.65, and 4.5 eV), and PVC+Cr_2O_3 (E_g=3.0 and 4.2 eV). The presence of NPs (Co_3O_4, NiO, and Cr_2O_3) in the PVC matrix produces these distinct energy gap values. It is worth noting that the energy gap has multiple values, which can be attributed to the influence of domperidone and the NPs on the PVC structure. The reduction in the energy gap is associated with the effective dispersion of domperidone and NPs within the PVC structure. Table 2 provides a summary of the optical energy gap values. Table 2 displays the values of the direct energy gap for pristine PVC, domperidone-modified PVC (PVC/D), and PVC nanocomposites (PVC/D/Co_3O_4, NiO, and Cr_2O_3).

Table 2: Direct energy gap.

Parameters	Pristine PVC	PVC/D	PVC/D/ Co_3O_4	PVC/D/NiO	PVC/D/ Cr_2O_3
Direct transition of (E_g) (eV)	4.7	3.0 and 4.0	3.6 and 4.7	3.5, 3.65, and 4.5	3.0 and 4.2

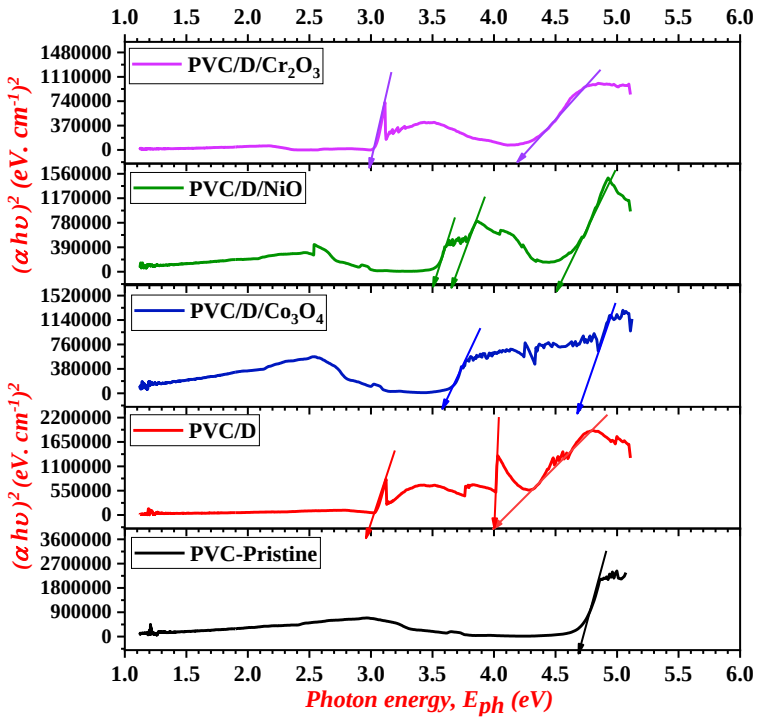

Figure 11: Optical energy gap/direct transition (*Eg*) for pristine PVC, modified PVC/D, and PVC/D/NPs.

Additionally, Figure 12 illustrates the curves of indirect transition for pristine PVC, domperidone-modified PVC (PVC/D), and PVC nanocomposites (PVC/D/Co_3O_4, NiO, and Cr_2O_3).

Figure 12 illustrates the indirect transition optical E_g for different materials: pristine PVC (E_g=4.3 eV), PVC+D (E_g=2.9 eV), PVC+Co_3O_4 (E_g=3.5 eV), PVC+NiO (E_g=3.4 and 3.9 eV), and PVC+Cr_2O_3 (E_g=3.0 and 3.7 eV). Adding domperidone with NPs (Co_3O_4, NiO, and Cr_2O_3) strengthens the PVC matrix and reduces the energy gap, as seen in the figures. The values of the indirect energy gap are summarized in Table 3 for reference [44]. Table 3 displays the values of the indirect energy gap for pristine PVC, domperidone-modified PVC (PVC/D), and PVC nanocomposites (PVC/D/Co_3O_4, NiO, and Cr_2O_3).

3.11. Urbach energy of PVC thin films

The localized states that are found in the band gap for any thin film have a relation directly to Urbach energy (E_u). These localized states lead to a disorder inside the material. Then, equation 9 is used to compute Urbach energy (E_u) [45].

$$\alpha=\alpha_o \exp\frac{h\nu}{E_u} \quad (9)$$

where, α_o: constant, E_u Urbach energy.

To arrange equation 9 to compute Urbach energy (E_u) from the slope of curves by taking the logarithm for the two sides and gain equation 10 [45].

$$\ln\alpha=\ln\alpha_o+\frac{h\nu}{E_u} \quad (10)$$

Table 3: Indirect energy gap.

Parameters	Pristine PVC	PVC/D	PVC/D/ Co_3O_4	PVC/D/NiO	PVC/D/ Cr_2O_3
Direct transition of (E_g) (eV)	4.3	2.9	3.5	3.4 and 3.9	3.0 and 3.7

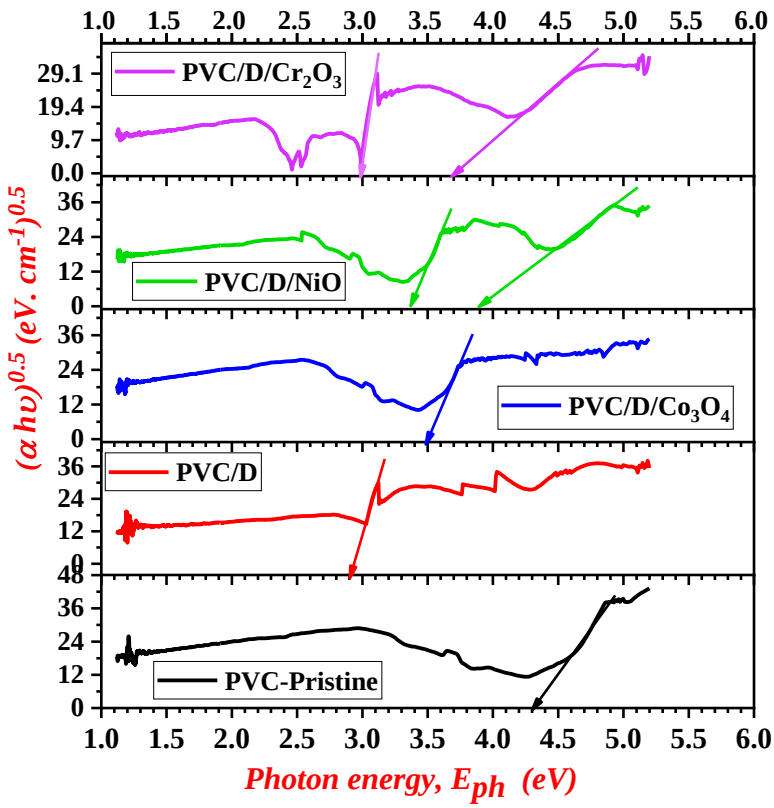

Figure 12: Optical energy gap/indirect transition (*Eg*) for pristine PVC, modified PVC/D, and PVC/D/NPs.

Figure 13 provides the Urbach energy (E_u) for various materials, including pristine PVC, modified PVC with organic compound (domperidone) (PVC/D), and PVC nanocomposites doped with NPs (Co_3O_4, NiO, and Cr_2O_3). The Urbach energy values can be calculated from the slope of the curves, as shown in Figure 13, and are used to characterize the localized states and disorder within the material. The specific values of *Eu* for each material can be obtained from Figure 13 [45].

Figure 13 depicts the *Eu* curves for pristine PVC, modified PVC with organic compound (domperidone) PVC/D, and PVC nanocomposites doped with Co_3O_4, NiO, and Cr_2O_3. These curves reveal that *Eu* increases for the nanocomposite thin films of modified PVC with domperidone. Specifically, the E_u values increase from 0.862 to 3.096 eV. This increase in *Eu* indicates an increase in localized states within the band gap and an increase in disorder within the material after adding organic compounds (domperidone) and NPs (Co_3O_4, NiO, and Cr_2O_3) to enhance the structure of PVC. Table 4 provides the results of α_o, E_u, and energy gap (direct and indirect transition) [46].

3.12. SEM of PVC thin films

As depicted in Figure 14, SEM images provide visual insights into the various PVC thin films. Figure 14a showcases a pristine PVC thin film, which appears smooth and uniform. In Figure 14b, a pristine PVC film modified with organic compound (domperidone) is observed, with organic compound (domperidone) visible as distinct spots within the film. Figure 14c illustrates the distribution of Co_3O_4 within the pristine PVC thin film modified with domperidone. Figure 14d displays the distribution of NiO with an organic compound (domperidone) within the pristine PVC thin film. This image reveals the formation of a porous structure in the film, intended to enhance its performance. Figure 14e demonstrates the distribution of chromium oxide nanoparticles Cr_2O_3 with organic compound (domperidone) distributed within the pristine PVC thin film. Similar to Figure 14d, this image also shows the formation of a porous structure within the film for improved performance of light absorbance [47, 48].

3.13. AFM inspection of PVC thin films

AFM analysis was employed to investigate the surface topography of the pristine PVC, modified PVC with domperidone (PVC/D), and the PVC nanocomposites (PVC/D/Co_3O_4, NiO, and Cr_2O_3). These AFM images provide insights into surface roughness, and the results are quantified in terms of average roughness and root mean square (RMS) values. Notably, the addition of domperidone and NPs (Co_3O_4, NiO, and Cr_2O_3) led to an increase in surface roughness, as reflected in the AFM images and summarized in Table 5, which presents the values of roughness and RMS for all PVC samples [49, 50]. Also, the study films' AFM 2D and 3D images are depicted in Figure 15.

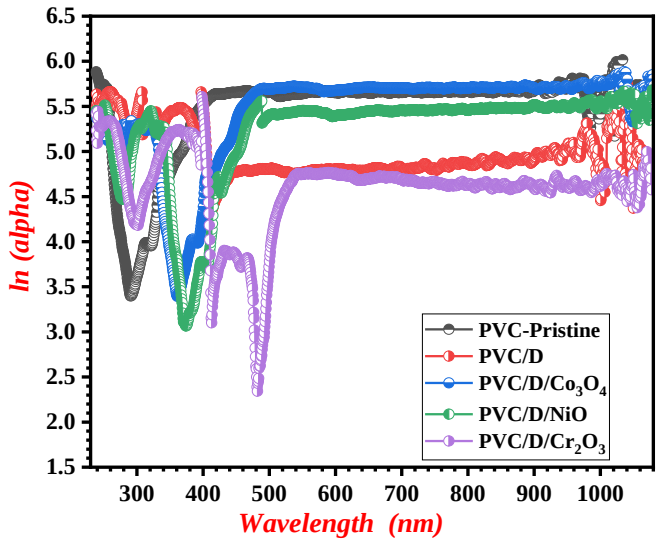

Figure 13: Urbach energy (E_u) for pristine PVC, modified PVC/D, and PVC/D/NPs.

Table 4: Band gap (direct and indirect), *Eu*, and α_o constant values.

No.	Essential parameters	Pristine PVC	PVC/D	PVC/D/Co_3O_4	PVC/D/NiO	PVC/D/Cr_2O_3
1	The direct transition of (E_g) eV	4.7	3.0 and 4.0	3.6 and 4.7	3.5, 3.65, and 4.5	3.0, 4.2
2	The indirect transition of (E_g) eV	4.3	2.9	3.5	3.4 and 3.9	3.0 and 3.7
3	Urbach energy (E_u) eV	0.862	0.885	0.909	3.096	2.650
4	α_o constant (cm^{-1})	87.71	110.72	113.86	178.22	96.16

Table 5: AFM explanation to the pristine PMMA and PMMA nanocomposite films.

No.	Composite	Figure's number	Roughness average (nm)	Root mean square of roughness (nm)
1	PVC-Pristine	15-a	2.31	3.07
2	PVC+D	15-b	2.93	4.02
3	PVC+D+Co_3O_4	15-c	4.04	5.41
4	PVC+D+NiO	15-d	3.72	4.87
5	PVC+D+Cr_2O_3	15-e	6.16	7.58

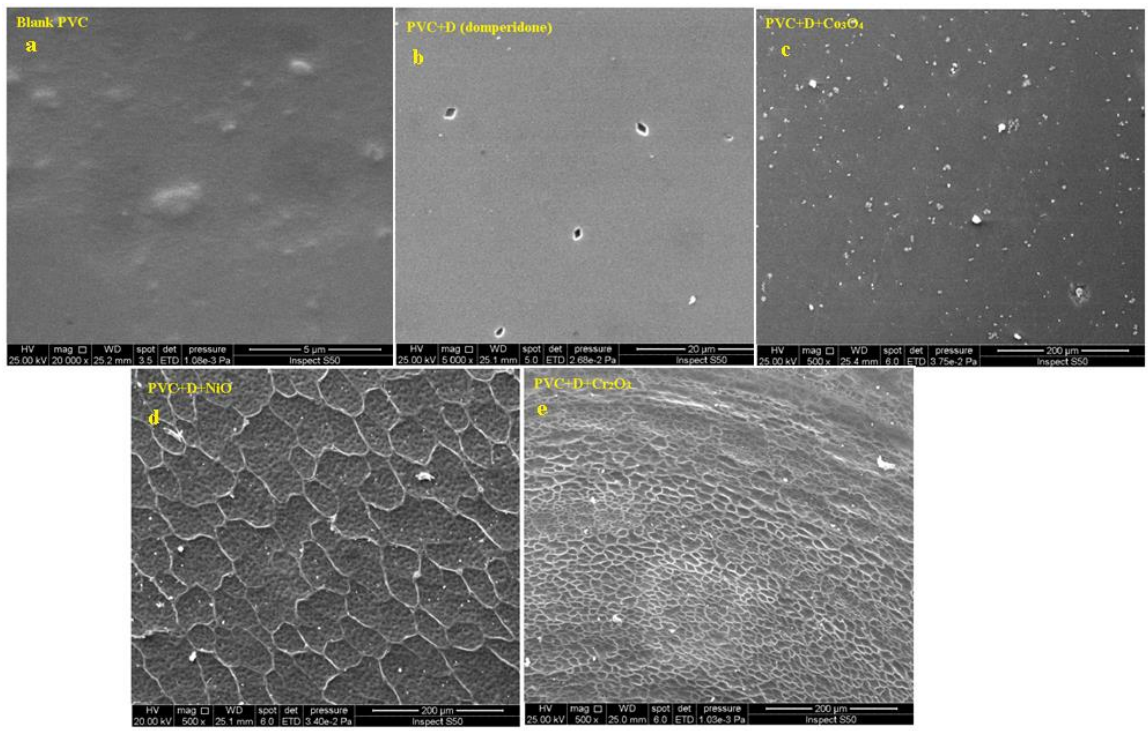

Figure 14: SEM images for a) blank-PVC, b) PVC+ organic compound (D), c) PVC+D+Co_3O_4, d) PVC+D+NiO, and e) PVC+D+Cr_2O_3.

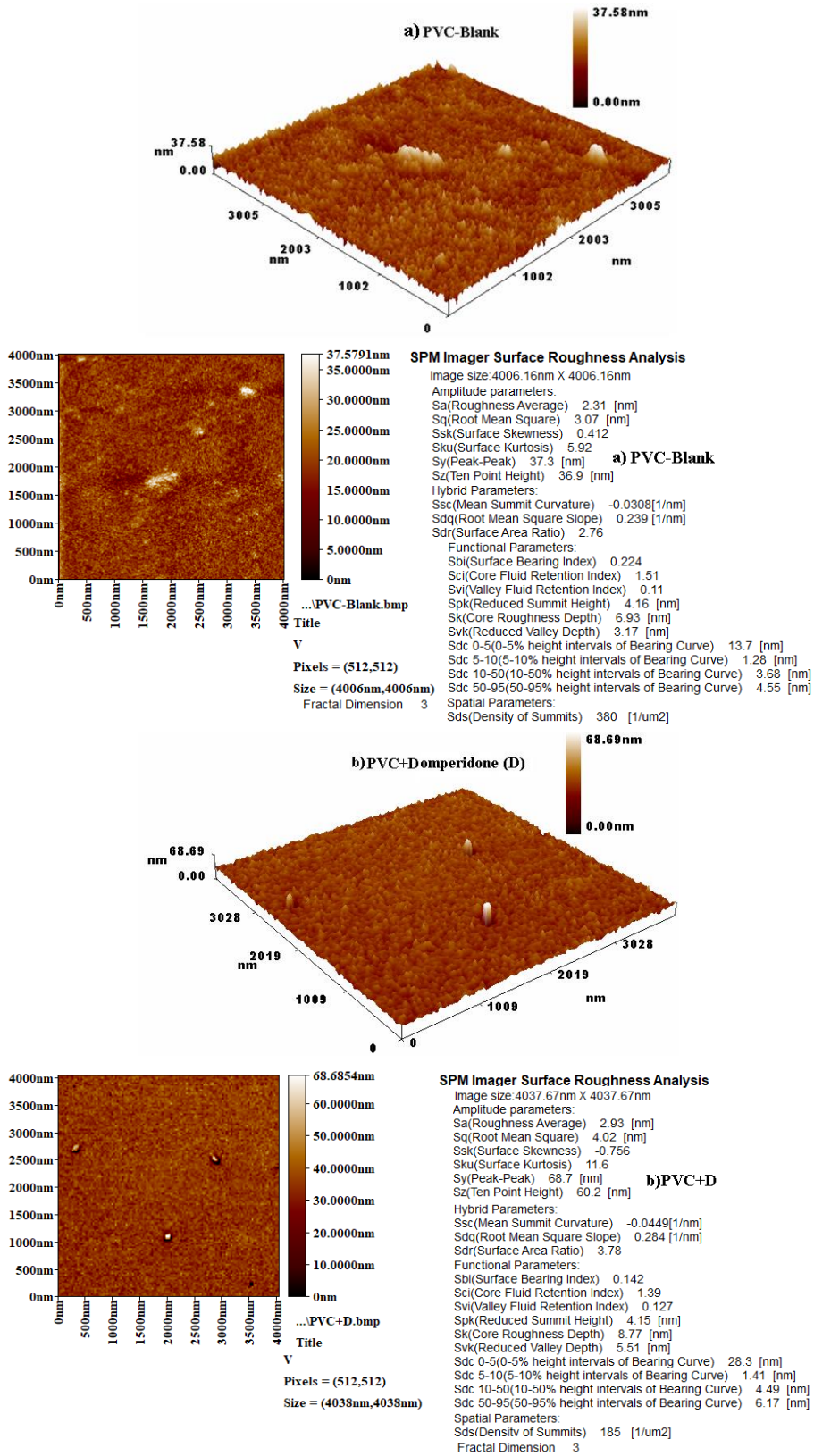

Figure 15: 2D and 3D AFM pictures of: a) blank-PVC, b) PVC+domperidone (D), c) PVC+D+Co_3O_4, d) PVC+D+NiO, and e) PVC+D+Cr_2O_3.

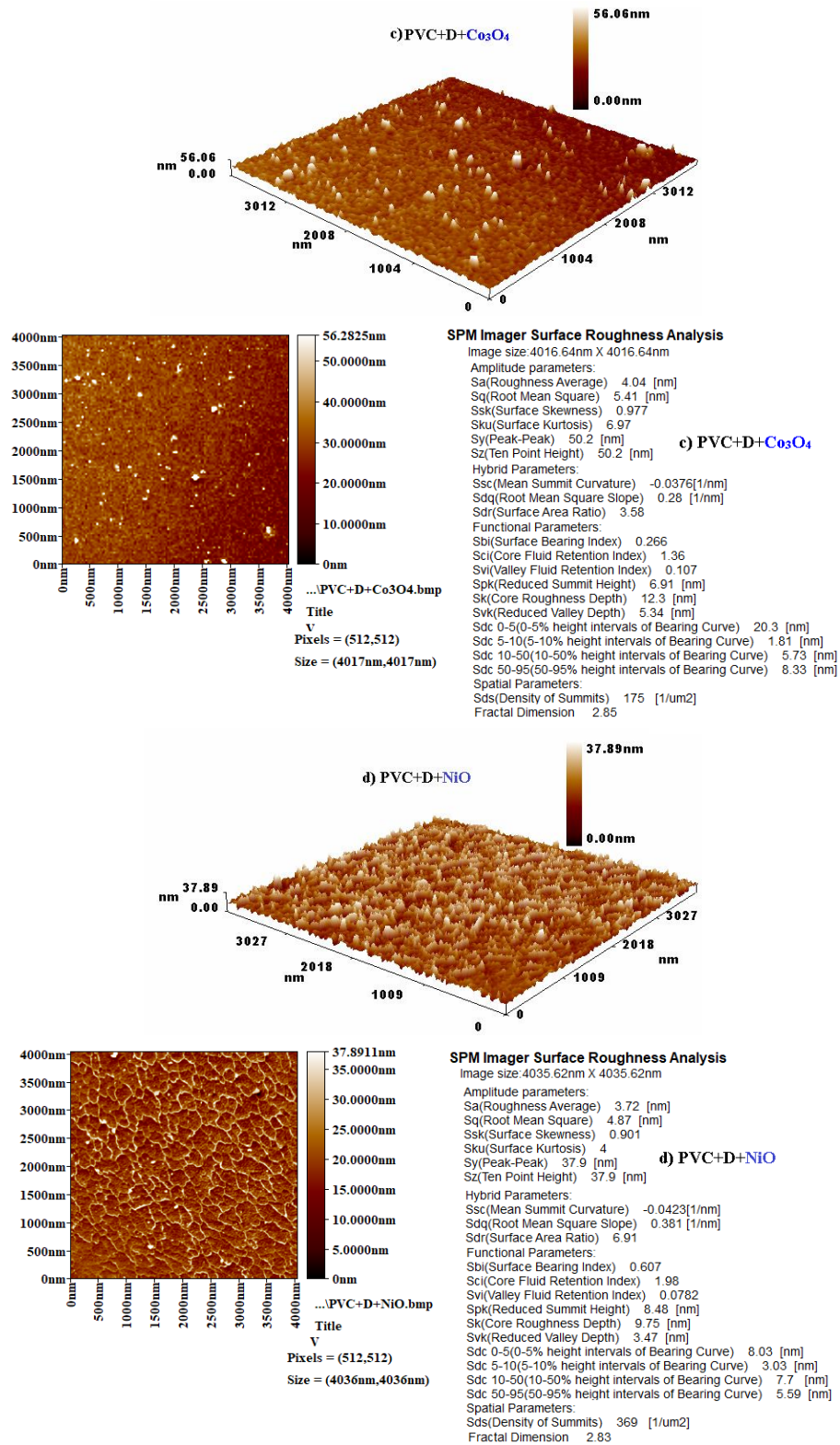

Figure 15: Continue.

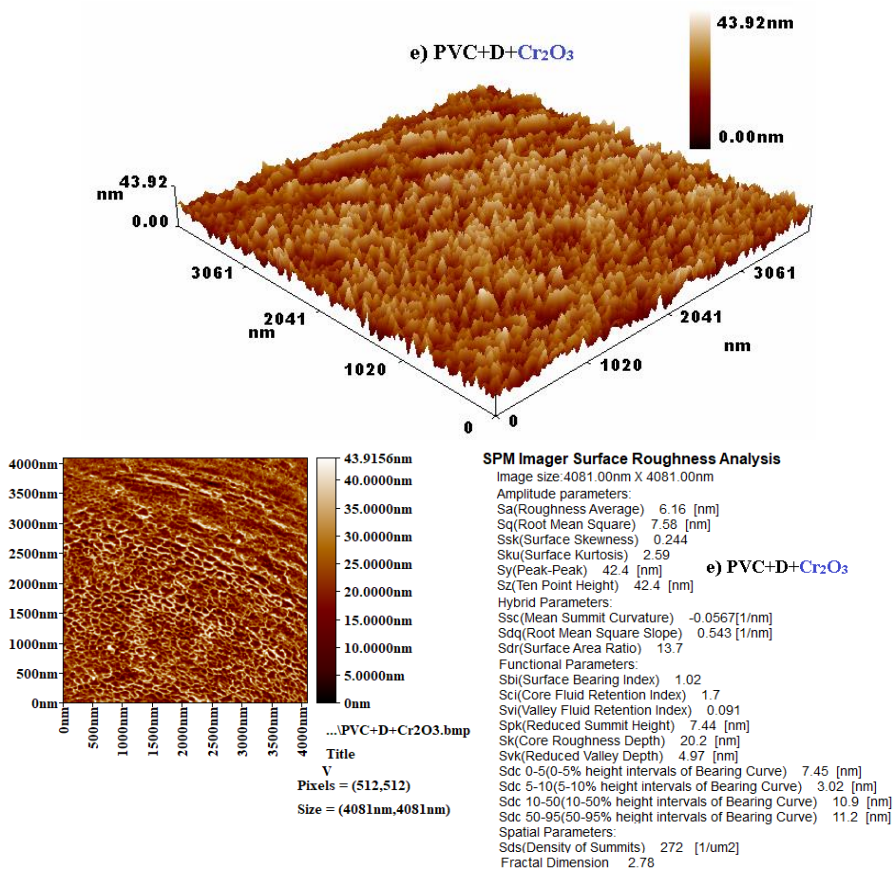

Figure 15: Continue.

3.14. Valence and conduction band

The direct and indirect energy gap of pristine PVC, modified PVC with organic compound (domperidone) PVC/D, and PVC nanocomposites doped with NPs (Co_3O_4, NiO, and Cr_2O_3) therefore Figures 16 and 17 display the photon energy gap declines between the valence and conduction band after additive the organic compound (domperidone) and the nanomaterials oxides as a dopant of the PVC matrix. The Figures 16 and 17 display the impact of the additives that altered the PVC structure as a host material for the selective surfaces used in light conversion industries [51].

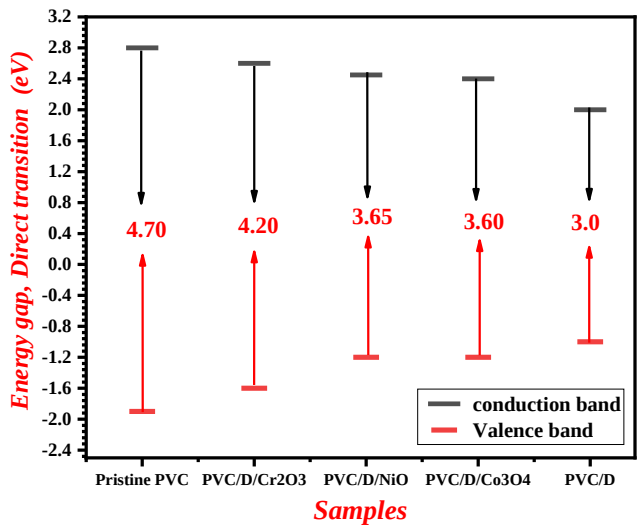

Figure 16: Direct energy gap transition of the pristine PVC, modified PVC/D, and PVC/D/NPs.

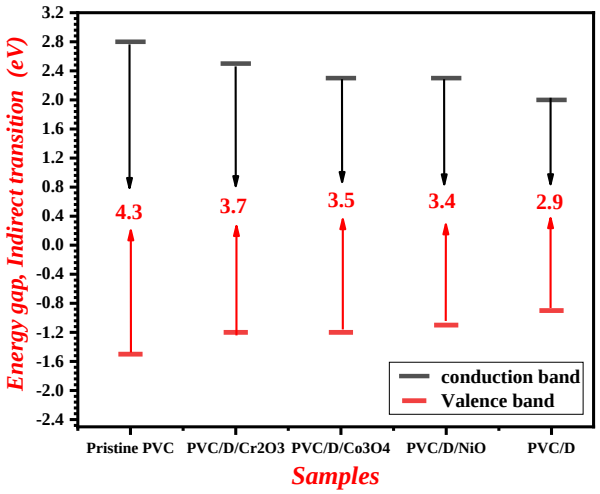

Figure 17: Indirect energy gap transition of the pristine PVC, modified PVC/D, and PVC/D/NPs.

4. Conclusion

In this study, novel modified nanocomposite thin films of PVC were successfully synthesized. The process involved dissolving 6 g of PVC in 100 mL of THF and modifying it with 25 g of domperidone, followed by doping with 0.01 g of nanoparticles (Co_3O_4, NiO, and Cr_2O_3). Various optical properties of these nanocomposite thin films were examined over a wide wavelength range (250-1350 nm). XRD testing revealed the formation of a semi-crystalline structure in the nanocomposite thin films. Transmittance (T) and reflectance (R) results indicated a decrease, while the absorption coefficient (α) increased to a range between 88-94%. The refractive index (n), optical conductivity (σ), and real dielectric constant (ε_1) increased, which suggested effective dispersion of domperidone and NPs within the PVC matrix. The lower values of the imaginary dielectric constant (ε_2) imply high absorption in these nanocomposite films. The direct and indirect energy gaps decreased from 4.7 to 3.0 eV and 4.3 to 2.9 eV upon doping with nanoparticles, indicating effective deposition of domperidone and NPs. *Eu* increased from 862.07 to 3095.97 meV, indicating an increase in localized states and disorder within the material. SEM and AFM analyses provided visual evidence of the modified PVC nanocomposite structure and increased roughness. These modified PVC nanocomposite thin films hold potential for various applications in industries such as air transport, light-emitting diodes, laser sensors, UV shields, light harvesting, memory devices, and light-converting devices.

Acknowledgments

The authors would like to express their gratitude for the collaborative support of the Department of Mechanical Engineering in the College of Engineering and the Department of Chemistry in the College of Science at Al-Nahrain University. This collaboration was instrumental in the completion of the current work.

5. References

1. Abed R N, Kadhom M, Ahmed D S, Hadawey A, Yousif E. Enhancing Optical Properties of Modified PVC and Cr_2O_3 Nanocomposite. Trans Electr Electron Mater. 2021; 22:317-327. https://doi.org/10.1007/s42341-020-00242-8.
2. Omer R M, Al-Tikrity E T B, Abed R N, Kadhom M, Jawad A H, Yousif E. Electrical conductivity and surface morphology of PVB films doped with different nanoparticles. Prog Color Colorant Coat. 2022; 15:191–202. https://doi.org/10.30509/PCCC. 2021. 81718.
3. Al-Daeif Y, Yousif E and Abdul Nabi M. Synthesis of new polymers derived from poly (vinyl chloride) and study their optical properties. ANJS 2012; 15:79-83. https://doi.org/10.22401/JNUS.15.2.10.
4. Ameer AA, Abdallh MS, Ahmed AA, Yousif EA. Synthesis and characterization of polyvinyl chloride chemically modified by amines open. J Poly Chem 2013; 3:3-11. https://doi.org/10.4236/ojpchem.2013.31003.
5. Abdallh M, Bufaroosha M, Ahmed A, Ahmed DS, Yousif E. Modification of poly(vinyl chloride) substrates via schiff's base for photochemical applications. J Vinyl Addit Technol. 2020; 26:475-480. https://doi.org/10.1002/vnl.21762
6. Yousif EA, Hameed AS, Emaad TB. Synthesis and photochemical study of poly(vinyl chloride)-1,3,4-oxadiazole and 1,3,4-thiadiazole. ANJS. 2007; 10:7-12. https://doi.org/10.22401/JNUS.10.1.04.
7. Abdallh MS. Synthesis and optical properties study of some metal complexes of poly(vinyl chloride)-pyridine-4-carbohydrazide. ANJS. 2013; 16:24-29. https://doi.org/10.22401/JNUS.16.2.04.
8. Yousif E, Abdallh M, Hashim H, Salih N, Salimon J, Abdullah BM, et al. Optical properties of pure and modified poly(vinyl chloride). Int J Ind Chem. 2013; 4:1-8. https://doi.org/10.1186/2228-5547-4-4
9. Yousif E, Ahmed DS, Ahmed AA, Hameed AS, Muhamed SH, Yusop RM, et al. The effect of high UV radiation exposure environment on the novel PVC

polymers. Environ Sci Pollut Res. 2019; 26:9945-9954. https://doi.org/10.1007/s11356-019-04323-x
10. Abdullah SM, Alwan AF, Majeed AM. The influence of the UV light on the PVC sheets adopted with some aromatic amines. ANJS. 2022; 25: 9-13. https://doi.org/10.22401/ANJS.25.1.02.
11. Yousif E, Abdallh M, Hashim H, Ahmed A, Ahmed DS, Yusop RM, Ahmed AA. Enhancement of the photo-chemical properties and efficacy of the mixing technique in the preparation of Schiff base-Cu(II)/poly(vinyl chloride) compounds. Emerg Mater Res. 2019; 2:505-512. https://doi.org/10.1007/s42247-019-00059-z.
12. Ahmed A. Synthesis and modified of poly(vinyl chloride) contains triazole moieties and studying the optical properties of new polymers. ANJS. 2015; 18:66-73, 2015. https://doi.org/10.22401/JNUS.18.1.09.
13. Abed RN, Yousif E, Abed ARN, Rashad AA, Hadawey A, Jawad AH. Optical properties of PVC composite modified during light exposure to give high absorption enhancement. J Non-Crys Solids. 2021; 570:120946. https://doi.org/10.1016/j.jnoncrysol. 2021. 120946.
14. Coiai S, Passaglia E, Pucci A, Ruggeri G. Nanocomposites based on thermoplastic polymers and functional nanofiller for sensor applications. J Mater. 2015; 8:3377-3427. https://doi.org/10.3390/ma8063377
15. Abdullah AM, Alwan LH, Ahmed AA, Abed RN. Optical properties of polystyrene with carbon nanotube and carbon nano incorporated and surface morphology studies. Int Nano Lett. 2023; 13:165–176. https://doi.org/10.1007/s40089-023-00398-0.
16. El Sayed AM, Morsi WM. Dielectric relaxation and optical properties of polyvinyl chloride/lead monoxide nanocomposites. Wiley 2013; 34:2031-2039. https://doi.org/10.1002/pc.22611.
17. Abed RN, Abed ARN, Abed AN, Electrical conductivity of carbon ash surface immersed with nanoparticles (Co_3O_4-Cr_2O_3) for spectroscopic selective surfaces. Poly Bull. 2023; 80:11207-11224. https://doi.org/10.1007/s00289-022-04601-8.
18. Hussein MA, Alam MM, Asiri AM, Al-amshany ZM, Hajeeassa KS, Rahman MM. Ultrasonic-assisted fabrication of polyvinyl chloride/mixed graphene-carbon nanotube nanocomposites as a selective Ag^+ ionic sensor. J Comp Mater. 2019; 53:2271–2284. https://doi.org/10.1177/0021998318825293.
19. Omer RM., Yousif E, Al-Tikrity ETB, Ahmed DS, Ali AA, Abed RNA. Detailed examination of UV radiation effects on the structural and morphological properties of polyvinyl butyral films containing different nanoparticles. Prog Color Colorant Coat. 2021; 14:209-219. https://doi.org/10.30509/PCCC.2021.81718
20. Yousif E, Al-Taa'y A, Noaman R, Esmael B, Abdalameer J, Abbas Q, et al. Effect of nano TiO_2 on the optical properties of PVC contains triazole moieties. YJES. 2016; 12:1437 H 21-27. https://doi.org/10.53370/ 001c.24308.
21. Ebnalwaled AA, Thabet A. Controlling the optical constants of PVC nanocomposite films for optoelectronic applications. Synth Met. 2016; 220:374-383. https://doi.org/10.1016/j.synthmet.2016.07.006.
22. Dadoosh RM, Alwan AF, Farhan SA, Jassim BE, Mahmood A, Al-Saadi LG, et al. Study of physicochemical properties of PVC thin films affected by carbon nanotubes to prevent photodegradation during UV light exposure. Prog Color Colorant Coat. 2024; 17:307-324. https://doi.org/ 10.30509/pccc.2024.167260.1275.
23. Abdallh M, Hamood O, Yousif E. Study the optical properties of poly (vinyl alcohol) doped cupper chloride. ANJS, 2013; 16:17-20. https://doi.org/ 10.22401/JNUS.16.1.03.
24. Mohammed SA, Yusop RM, Abdulsattar M, Abed RN, Ahmed DS, Ahmed A, et al. Additives aid switch to protect the photodegradation of plastics in outdoor construction. NJES. 2019; 22:277-282. http://doi.org/10. 29194/ NJES.22040277.
25. Abed RN, Zainulabdeen K, Abdallh M, Yousif E, Rashad AA, Jawad AH. The optical Properties Behavior of Modify Poly(Methyl Methacrylate) Nanocomposite Thin Films during solar energy absorption. J Non-Cryst Solid. 2023; 609:122257. https://doi.org/10.1016/j.jnoncrysol.2023.122257.
26. Hassanien AS, Aly KA, Elsaeedy HI, Alqahtani A. Optical characterization and dispersion discussions of the novel thermally evaporated thin a-S50-xGe10CdxTe40 films. Appl Phys.A. 2022; 128: 1021. https://doi.org/10.1007/s00339-022-06127-2.
27. Abed RN, Abed ARN, Khamas FA, Abdallh M, Yousif E. High performance thermal coating comprising (CuO:NiO) nanocomposite/C spectrally selective to absorb solar energy. Prog Color Colorant Coat. 2020; 13:275-284. https://doi.org/10.30509/PCCC.2020.81662.
28. Abdullah AM, Alwan LH, Ahmed AA, Abed RN. Optical and physical properties for the nanocomposite poly(vinyl chloride) with affected of carbon nanotube and nano carbon. Prog Color Colorant Coat. 2023; 16:331-345. https://doi.org/10.30509/PCCC.2023.167082. 1198.
29. Hadi, AG, Jawad K, El-Hiti GA, Alotaibi MH, Ahmed AA, Ahmed DS. et al. Photostabilization of poly(vinyl chloride) by organotin(IV) compounds against photodegradation. Molecules. 2019; 24: 3557, 1-15. https://doi.org/10.3390/molecules24193557.
30. Mariappan R, Ponnuswamy V, Ragavender M. Characterization of $CdS_{1-x}Se_x$ thin films by chemical bath deposition technique. Optik. 2012; 123:1196-1200. https://doi.org/10.1016/j.ijleo.2011.07.050.
31. Dolai S, Sarangi SN, Hussain S, Bhar R, Pal AK. Magnetic properties of nanocrystalline nickel incorporated CuO thin films. J Magn Magn Mater. 2019; 479:59-66. https://doi.org/10.1016/j.jmmm.2019.02.005.
32. Abdullah AM, Alwan LH, Ahmed AA, Abed RN. Physical study of PVA filled with carbon nanotube and

nano carbon with roughness morphology. J Phys Chem Res. 2023; 11:747-760. https://doi.org/10.22036/ PCR.2022.362088.2195.
33. Abed RN, Al-Sahib NK, Khalifa AJN. Energy gap demeanor for carbon doped with chrome nanoparticle to increase solar energy absorption. Prog Color Colorant Coat. 2020; 13:143-154. https://doi.org/10. 30509/ PCCC.2020.81613.
34. Al-Bataineh QM, Alsaad AM, Ahmad AA, Al-Sawalmih A. Structural, electronic and optical characterization of ZnO thin film-seeded platforms for ZnO nanostructures: sol-gel method versus Ab iInitio calculations. J Electron Mater. 2019; 48:5028-5038. https://doi.org/10.1007/s11664-019-07303-6.
35. Abed RN, Abed ARN, Yousif E. Carbon surfaces doped with (Co_3O_4-Cr_2O_3) nanocomposite for high-temperature photo thermal solar energy conversion via spectrally selective surfaces. Prog Color Colorant Coat. 2021; 14:301-315. https://doi: 10.30509/pccc.2021. 166749.1098.
36. Abed RN, Abdallh M, Rashad AA, Hadawey ., Yousif E. New coating synthesis comprising CuO:NiO/C to obtain highly selective surface for enhancing solar energy absorption. J Polym Bull. 2021; 78:433-455. https://doi.org/10.1007/s00289-020-03115-5
37. Pankove JI. Optical Processes in Semiconductors, book, Dover Publications Inc., New York, NY, USA 1975. p. 91.
38. Ahmed A, Abed RN, Kadhom M, Hashim H, Akram E, Jawad A, et al. Modification of poly (vinyl chloride) thin films with organic compound and nanoparticles for solar energy applications. J Polym Res. 2023; 30. https://doi.org/10.1007/s10965-023-03654-1.
39. Abed RN, Yousif E, Abed ARN, Rashad AA. Synthesis thin films of poly(vinyl chloride) doped by aromatic organosilicon to absorb the incident light. Silicon. 2022; 14:11829-11845. https://doi.org/10.1007/ s12633-022-01893-3.
40. Abed RN. Al-Mashhadani MH, Yousif E, Hashim H, Yusop RM, Bufaroosha M. Organosilane-doped PVC lattice thin film for optoelectronic applications. J Opt. 2023. https://doi.org/10.1007/s12596-023-01351-2
41. Fasasi A, Osagie E, Pelemo D, Obiajunwa E, Ajenifuja E, Ajao J, et al. Effect of precursor solvents on the optical properties of copper oxide thin films deposited using spray pyrolysis for optoelectronic applications. Am J Mater Synth Process. 2018; 3:12-22. https://doi.org/10.11648/j.ajmsp.20180302.12.
42. Souri D, Tahan ZE. A new method for the determination of optical band gap and the nature of optical transitions in semiconductors. Appl Phys B. 2015; 119:273-279. https://doi.org/10.1007/s00340-015-6053-9.
43. Alsaad AM, Al Bataineh QM, Ahmad AA, Albataineh Z, Telfah A. Optical band gap and refractive index dispersion parameters of boron-doped ZnO thin films: a novel derived mathematical model from the experimental transmission spectra. Optik. 2020; 211: 164641. https://doi.org/10.1016/j.ijleo. 2020. 164641
44. Abdullah AM, Alwan LH, Ahmed AA, Abed RN, Optical and physical properties for the nanocomposite poly(vinyl chloride) with affected of carbon nanotube and nano carbon. Prog Color Colorant Coat. 2023; 16:331-345. https://doi.org/10.30509/PCCC.2023. 167082. 1198.
45. Hassanien A., Akl AA. Effect of Se addition on optical and electrical properties of chalcogenide CdSSe thin films. Superlattice Microst. 2016; 89:153-169. https://doi.org/10.1016/j.spmi.2015.10.044.
46. Abed RN, Sattar MA, Hameed SS, Ahmed DS, Al-Baidhani M, Kadhom M. Optical and morphological properties of poly(vinyl chloride)-nano-chitosan composites doped with TiO_2 and Cr_2O_3 nanoparticles and their potential for solar energy applications. Chem Papers. 2023; 77: 757-769. https://doi.org/10.1007/ s11696- 022- 02512-6.
47. Abed ARN, Abed RN. Characterization effect of copper oxide and cobalt oxide nanocomposite on poly(vinyl chloride) doping process for solar energy applications. Prog Color Colorant Coat. 2022; 15:235-241.https://doi.org/10.30509/PCCC.2021.166858.1123.
48. Hassanien AS, Neffati R, Aly KA. Impact of Cd-addition upon optical properties and dispersion parameters of thermally evaporated $Cd_xZn_{1-x}Se$ films: Discussions on bandgap engineering, conduction and valence band positions. Optik. 2020; 212:164681. https://doi.org/10.1016/j.ijleo.2020.164681.
49. Hassanien AS, Akl AA, El Redaf IM. Optical characteristics of the novel nanosized thin $ZnGa_2S_4$ films sprayed at different deposition times: Determination of optical band-gap energy using different methods. Emergent Mater. 2023; 6:943-964. https://doi.org/10.1007/s42247-023-00493-0.
50. Hassanien AS, El Radaf IM. Effect of fluorine doping on the structural, optical, and electrical properties of spray deposited Sb_2O_3 thin films. Mater Sci Semicond Proc. 2023; 160:107405. https://doi.org/10.1016/j.mssp. 2023.107405.
51. Emir P, Kuru D. Boron nitride quantum dots/polyvinyl butyral nanocomposite films for the enhanced photoluminescence and UV shielding properties. J Appl Polym Sci. 2024; 141:55171. https://doi.org/10. 1002/ app.55171.

How to cite this article:
Abed RN, Yousif E, Rahman MH, Kadhom M, Basem A, Hashim H. Optical and Morphological Properties of Poly(vinyl chloride) Thin Films with Organic Content Reinforced by Nanoparticles Embedded which is Freestanding. Prog Color Colorants Coat. 2025;18(2):145-162. https://doi.org/ 10.30509/pccc.2024.167313.1300.